FACTA UNIVERSITATIS
Series: **Electronics and Energetics** Vol. 34, Nº 4, December 2021, pp. 605-630
https://doi.org/10.2298/FUEE2104605A

Original scientific paper

EFFECTS OF CONNECTING A SCATTERED SOLAR GENERATION UNIT TO THE GRID ON THE CLOUD PASSAGE USING OPTIMIZATION ALGORITHMS

Ali Aljbori, Mahdi Zarif

Department of Electrical Engineering, Mashhad Branch, Islamic Azad University, Mashhad, Iran

Abstract. *Today, limitation of fossil fuel resources and other issues such as the possibility of the depletion of fossil energy reserves, global warming, environmental pollution, price instability, and the growing need for industrial and urban centers for energy have prompted the international community to seek appropriate alternatives. Such examples are nuclear energy, solar energy, geothermal energy, wind energy, and ocean waves. Renewable energy is generated owing to the simplicity of the applied technology compared to nuclear energy technologies. On the other hand, such energies play a key role in new energy systems in the world similar to nuclear waste. The increasing use of renewable energies has given rise to significant complications. One of the main operational issues in this regard is the uncertainty of electricity generation by solar power plants, which is caused by the passage of clouds. The present study aimed to investigate the effects of cloud passage on the production of solar power plants. Initially, a control system was designed to control a high-penetration solar power plant in the network, and the maximum allowable percentage of penetration was calculated for different loads. For this purpose, three algorithms (DE, PSO, and ICA) were used to determine the MPPT of the solar arrays in shady conditions, as well as the MPPT point of the solar arrays. According to the results, the colonial competition algorithm was faster compared to the other algorithms*.

Key words: *Photovoltaics, solar cells, Maximum Power Point Tracking, Particle Swarm Optimization, Differential Evolution, Imperialist Competitive Algorithm*

Received April 4, 2021; received in revised form June 25, 2021
Corresponding author: Ali Aljbori
Department of Electrical Engineering, Mashhad Branch, Islamic Azad University, Mashhad, Iran
E-mail: aljbori.a1989@gmail.com

1. INTRODUCTION

Today, limitation of fossil fuel resources and other factors such as the possibility of the depletion of fossil energy reserves, global warming, environmental pollution, price instability, and the growing need for industrial and urban centers for energy have prompted the international community to seek appropriate alternatives. Such examples are nuclear energy, solar energy, geothermal energy, wind energy, and ocean waves. On the other hand, atomic ions play a key role in new energy systems in the world. Despite the increasing demand for electricity and the growing need for high-quality and reliable electricity, lack of responsive production, distribution, and transmission infrastructures in large electricity networks in some cases has led to scattered energy resources for further development [1].

Use of distributed generation resources along with the supplying parts of the load increases the reliability of the power system through the proper placement of the distributed generation sources. Furthermore, losses could be decreased and voltage profiles could be improved, which ultimately lead to increased energy efficiency [2]. Solar energy is considered to be the most viable option among various scattered production sources given the problems associated with air pollution, as well as the abundance of high-power sunlight. A solar power plant is cost-efficient and able to cover a large portion of an area load (affecting air pollution) when it is large-scale in terms of energy production. Scattering provides a significant amount of load to a feeder, which also known as a high-penetration scattering source. The use of high-penetration solar power plants in the distribution network has numerous advantages and several technical disadvantages.

Ohmic voltage drop in distribution networks is an important issue, and pulsed transformers are used for its compensation. Distribution lines are mostly radial and designed to flow in one direction. By inserting a high-penetration solar power plant into parts of the feeder, the flow direction is reversed, thereby reducing the current sent by the distribution substation and also causing a significant decline in the voltage drop across the distribution network. If hotline pulses that cannot change the transformer pulse under the load are not used in the feeder, the PCC voltage will be higher than usual .The issue becomes more acute when the consumed load during the day changes. Since the highest amount of electricity is generated by the solar power plant during the time with the lowest load consumption, the penetration of the power plant is maximized in this period. Therefore, the manual pulse changers currently used in distribution networks cannot be used for voltage regulation.

The effects of cloud passage may be highly destructive to the voltage and power balance in a distribution network. If the generation capacity of the solar power plant is partly comparable to the main power plant (steam, gas), the disturbance of the grid power balance could become problematic due to the instantaneous reduction of the generation power in the solar power plant. This occurs because a steam or gas power plant with a ramp could compensate for the reduction in the instantaneous production capacity, which may in turn cause power shortage in large parts of the network. In addition, the emergence of voltage fluctuations in the network could lead to customer dissatisfaction or the inefficient operation of network equipment. To date, several studies have evaluated the connection of the photovoltaic system:

"Integrated Autonomous Voltage Regulation and Islanding Detection for High Penetration PV Applications". This paper proposes an autonomous unified var controller to address the system voltage issues and unintentional islanding problems associated with distributed photovoltaic (PV) generation systems. The proposed controller features the integration of both

voltage regulation (VR) and islanding detection (ID) functions in a PV inverter based on reactive power control [2].

"A Novel Approach for Ramp-Rate Control of Solar PV Using Energy Storage to Mitigate Output Fluctuations Caused by Cloud Passing". This paper proposes a strategy where the ramp-rate of PV panel output is used to control the PV inverter ramp-rate to a desired level by deploying energy storage (which can be available for other purposes, such as storing surplus power, countering voltage rise, etc) [3].

"A study of dispersed photovoltaic generation on the PSO system". Results of a study on dispersed photovoltaic (PV) generation on the Public Service Company of Oklahoma (PSO) system with simulated dispersed PV generation are presented [4].

"Influence of photovoltaic power generation on required capacity for load frequency control". in this paper developed a mathematical model to evaluate the impact of small (rooftop) photovoltaic (PV) power-generating stations on economic and performance factors for a larger scale power system, and applied this model to the Tokyo metropolitan area [5].

In all papers data are limited regarding the problems that could occur within the network; such examples are swing power, increased/decreased voltage profiles, failure of protection devices, cloud effect, power plant harmonics, and network frequency regulation [3-12].

The necessity of building and connecting to the solar power plant grids and the unforeseen issues that occur with the introduction of these power plants to the grid have motivated the current research.

The present study aimed to investigate the effects of connecting a scattered solar generation unit to the grid in the cloud passage and determined the feeder load changes for a fixed consumer from an operational perspective.

2. Materials and Methods

To date, several studies have evaluated the connection of the photovoltaic system to the network and various penetrations rates within a photovoltaic system in the electricity network. However, data are limited regarding the problems that could occur within the network; such examples are swing power, increased/decreased voltage profiles, failure of protection devices, cloud effect, power plant harmonics, and network frequency regulation [3-12].

In this study, we assessed the effects of connection to a high-penetration solar power plant in the distribution network in terms of voltage and the changes in the feeder load for a constant consumer from an operational perspective. By connecting the power plant to the distribution network, which had transformers with manual pulse changers that are unchangeable under load, the voltage at the end of the line and where the power plant was connected to the network increased.

The ANSI standards allow 4% overvoltage for distribution networks. Given that the impedance of distribution lines is higher than the standard value in some cases, it is paramount to investigate the effects of the overvoltage. On the other hand, the feeder is mainly powered by the solar power plant, and it is not an economical option to incorporate large amounts of energy storage in high-power plants. This is because by crossing the cloud and casting a shadow on solar array panels, their instantaneous power decreases significantly. The power reduction causes the power balance of the distribution network and the disturbance of the power plant, as well as voltage change. In this study, we also evaluated the effects of cloud transit by initially defining a photovoltaic system and a solar panel model.

2.1. Photovoltaic System [13-16]

Photovoltaics (PV) refer to a solar power generation system. In this method, solar cells are used for the direct production of electricity from solar radiation. These solar cells are semiconductors and composed of silicon. When sunlight shines on a photovoltaic cell, a potential difference occurs between the negative and positive electrodes, causing the current to flow in-between. PV could be classified as a renewable energy technology, and a photovoltaic system consists of several components and subsystems, including the photovoltaic effect manufacturer by mechanical tools, battery (energy storage subsystem), control equipment, monitors, and measurement devices, and support manufacturer.

2.2. Solar Panel Modeling [17]

The physical structure of a solar cell is similar to a diode the p-n junction of which is exposed to sunlight. The absorbed energy from the light intensity in this area leads to the production and transfer of carriers (electrons and holes) and their aggregation in the output terminal. A solar panel has several photovoltaic cells with a series of external connections (parallel or series-parallel). Figure 1 shows the function of a solar cell. Figure 2 depicts the equivalent circuit of a solar cell.

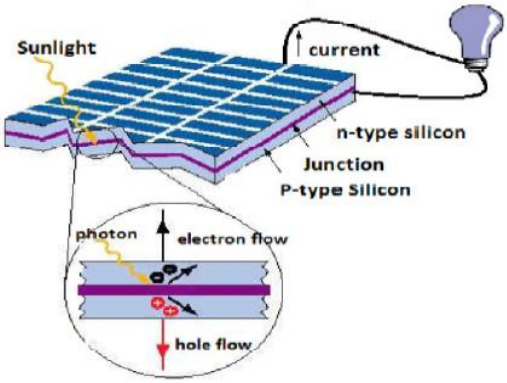

Fig. 1 Solar Cell Function [2, 4]

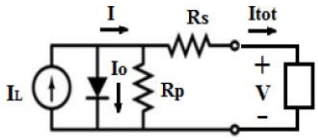

Fig. 2 Solar Cell Orbit Equivalence

In this study, the characteristics of the solar panel were determined based on the parameters of Equation 1 t0 3 as follows:

$$I = I_{ph} - I_o\left(e^{V_D/A.V_T} - 1\right) - \frac{V+R_sI}{R_p} \quad (1)$$

$$I_{ph} = S.\left(I_{sc} - \alpha(T - 25)\right) \tag{2}$$

$$P = VI = V(I_{ph} - I_o\left(e^{V_D/_{A.V_T}} - 1\right) - \frac{V+R_sI}{R_p}) \tag{3}$$

where q is the electron electric charge, K shows the Boltzmann constant, VT is the thermal voltage, T represents the absolute cell temperature (°K), A is the diode emission coefficient, Io shows the reverse saturation current, Iph is the photovoltaic component of the current, S is the sunlight (kw/m2), α shows the short-circuit current temperature coefficient, ISC is the cell short-circuit current under standard conditions (25°C, radiation: kw/m2), VD is the diode voltage, RS shows the series noise resistance, Rp is the parallel noise resistance, V is the solar cell terminal voltage, I shows the solar cell terminal current, and P represents the solar cell output power. If series resistance and parallel resistance (0≈Rs and pRp) are eliminated and the short-circuit conditions are considered, the source current of the model is approximately equal to the short-circuit current. Equation 4 was applied for the assessment of the solar cell.

$$I \approx I_{sc}(1 - e^{\frac{V-V_{OC}}{A.V_T}}) \tag{4}$$

Photovoltaic systems could be used to generate electricity in any setting with a high potential for the absorption of solar energy. Due to the high costs of solar cell production and the cost-efficiency of electricity generation by fossil fuels from photovoltaic systems, the national electricity grid is commonly used in remote areas (e.g., villages and borders). Other applications of these systems for street lighting in cities are as solar pumping systems using photovoltaic, portable solar, and power supply systems for telecommunication and seismic stations and tunnel lighting systems for mountain roads.

V-I. The characteristics of a temperature- and radiation intensity-based solar representation have been shown in Equations 5-11.

$$v_{SA} = \frac{N}{\lambda} ln\left(\frac{MI_{ph} - i_{SA} + MI_o}{MI_o}\right) - \frac{N}{M} R_S i_{SA} \tag{5}$$

$$\Delta T = T - T_r \tag{6}$$

$$\Delta i = \alpha(I_{sc} - I_{scr})\Delta T + \left(\frac{I_{sc}}{I_{scr}} - 1\right) I_{scr} \tag{7}$$

$$\Delta v = -\beta \Delta T - R_s \Delta i \tag{8}$$

$$v_{SA}^{new} = v_{SA} + \Delta v \tag{9}$$

$$i_{SA}^{new} = i_{SA} + \Delta v \tag{10}$$

$$P_{SA} = v_{SA}^{new} i_{SA}^{new} \tag{11}$$

In these equations, T and T_r are the working point temperature and the nominal temperature of a solar panel, respectively, α shows the coefficient of the temperature flow, β is the voltage coefficient of temperature, and T_{SC} and T_{SCr} represent the short-circuit current at the operating point and the name of the solar panel, respectively. For a silicon solar panel (N=36, M=1), Equation 5 will become Equation 12.

$$v_{SA} = k\ ln\left(\frac{I_{ph} - i_{SA} + I_o}{I_o}\right) - i_{SA} \tag{12}$$

In addition, the production current with a specific radiation level could be obtained using Equation 13.

$$I_{ph} = [I_{scr} + \alpha(T - T_r)] \cdot (S/1000) \tag{13}$$

Figure 3 shows the P-I characteristic of a radiation intensity-based solar array, and Figure 4 depicts the temperature-based solar array. By observing these curves, it could be concluded that the output power of a solar array is highly nonlinear and largely depends on the amount of radiation and the intensity of the ambient temperature. Therefore, these figures show that the maximum power point (MPP) would change with changes in the temperature and radiation intensity. To achieve the optimal operating point of the system, it is essential to use the MPPT algorithm.

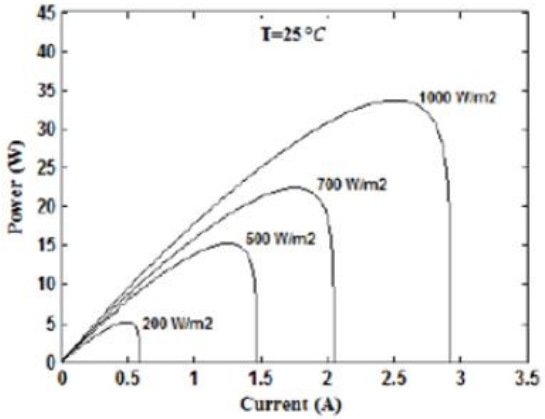

Fig. 3 The characteristics of the P-I solar arrays at a constant temperature and different radiation intensities [18-23]

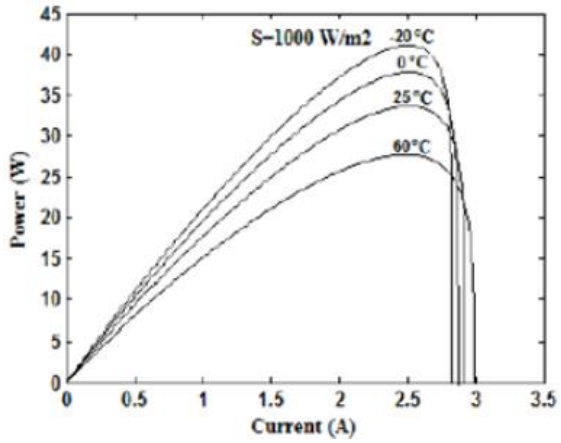

Fig. 4 The characteristics of the P-I solar arrays at a constant temperature and different radiation intensities [18-23]

2.3. Maximum Power Point Tracking (MPPT)Algorithm

To use a solar array at the maximum operating point, an MPPT method is required to detect the power peak. This method obtains the voltage and current at which the solar array has the maximum power in the output. Figures 5 and 6 show the characteristic curves of the V-I and P-I of a solar array at the radiation intensity of 1,000 W/m^2 and temperature of 25°C, respectively. Furthermore, these figures illustrate the characteristics of the solar array under partial shading conditions, which shows five cells with the radiation intensity of 800 W/m^2 and temperature of 23°C, as well as five cells with the radiation intensity of 500 W/m^2 and temperature of 25°C.

As is shown in Figures 5 and 6, many MPPT methods do not function properly under partial shadow conditions and the local optimal MPP point converges due to the presence of several peak points under shady conditions. To solve this issue, the MPPT algorithm could be used based on random optimization methods.

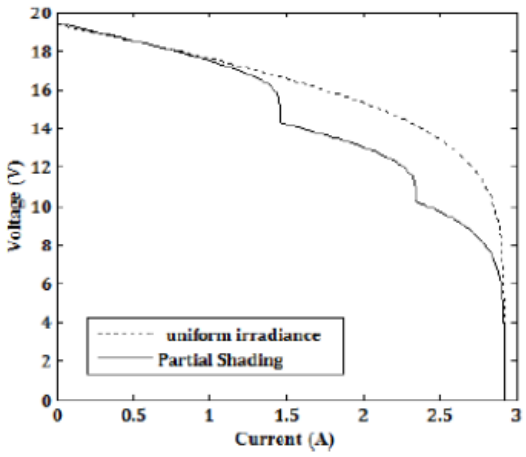

Fig. 5 V-I with and without Shadow [18-23]

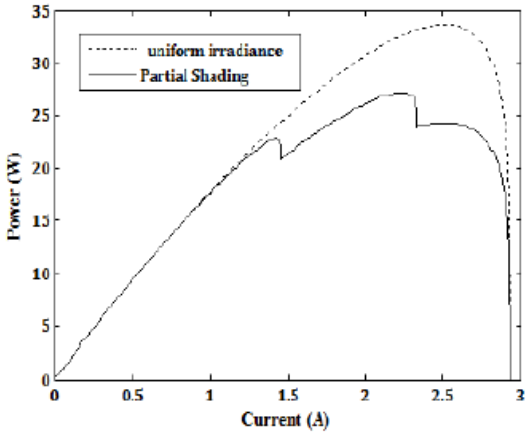

Fig. 6. P-I with and without Shadow [18-23]

2.3.1. MPPT-based Optimization Algorithm

The main advantage of stochastic optimization algorithms is escaping from the local optimal points. Stochastic optimization algorithms such as PSO and DE could detect the optimal point of a problem, which makes them useful in finding the maximum power point of solar arrays under shady conditions. We considered the output power of the solar array as the objective function of the optimization problem as in Equation 14.

Figure 7 shows the structure of the studied system. In this system, the tracker connects the maximum solar power of the PV module to the battery. The maximum power tracking system consists of a DC-DC converter and a PID control system and controller (PSO MPPT/DE MPPT). The PSO MPPT/DE MPPT unit uses environmental parameters at its input, along with Equations 5-13 to determine the voltage and current of the maximum power. The inputs of the MPPT method based on the stochastic optimization algorithm included T (cell temperature), S (radiation intensity), N_{shadle} (number of the cells in the shade), T_{shade} (temperature of the cells in the shade), and Sshade (radiation intensity in the cells in the shade).

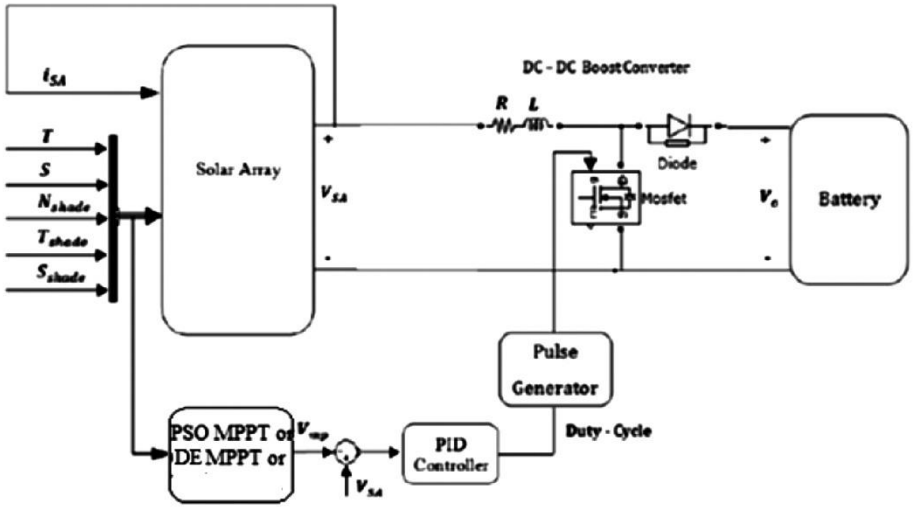

Fig. 7. Structure of Studied System

The maximum power tracking system could achieve the optimum operating power point of the maximum power supply (Pmax) by adjusting the Duty Cyck value of the skin converter. The DC-DC boost converter adjustment function based on its permanent state is as follows:

$$V_0 = \frac{V_{SA}}{1-d} \tag{14}$$

where d is the value of the life cycle, V_O shows the output voltage of the DC boost converter, and V_A is the output voltage of the solar array. The optimal value was calculated using Equation 14, in which V_{SA}=Vmp and V_0=25v (battery voltage). In this sections, we define the random algorithms used in the article.

2.3.2. Particle Swarm Optimization (PSO) Algorithm [24-25]

In the past decade, the particle swarm optimization (PSO) algorithm, which is based on stochastic research methodologies for general optimization, was proposed by Abr Hart et al. based on the models of simple social systems to solve nonlinear problems such as distribution optimization. Reactive power is highly efficient, and the characteristics of this algorithm have been further discussed. This algorithm is based on research on different communities (e.g., bird communities) and a very simple concept. Therefore, the time required for the calculations is very short and does not require considerable memory. In addition, the algorithm has been developed for nonlinear and continuous optimization problems, while it could also be used for problems with discrete variables.

2.3.3. Differential Evolution (DE) Algorithm [26-28]

Differential evolution (DE) is a simple population-based algorithm, which randomly searches for the optimal point of the network. This algorithm is able to optimize nonlinear and non-derivative target functions. In the DE algorithm, the populations include vectors with real values, and the key advantage of the algorithm is that it results in better answers compared to other methods at the same time.

2.3.4. Imperialist Competitive Algorithm (ICA) [29-30]

The Imperialist Competitive Algorithm (ICA) is an evolutionary computational method, which determines the optimal answers to various optimization problems. The algorithm provides an algorithm for solving mathematical optimization problems by mathematically modeling the process of social and political evolution In terms of application, the ICA is classified as an evolutionary optimization algorithm similar to the genetic algorithm (GA), PSO, and Ant Colony Optimization (ACO). The main advantage of the imperialist competition algorithm is its high speed compared to other optimization algorithms.

2.4. Microgrids [31]

Microgrids are low-voltage electrical networks consisting of scattered energy sources such as microturbines, solar cells, wind turbines, and fuel cells. Moreover, microgrids include energy storage equipment such as batteries and flywheels, as well as controllable loads. Microgrids could be used when connected to the grid and when disconnected from the grid, which greatly increases the reliability of the delivered energy. Connecting any sources (microgrids) to a distributed generation system (except conversion from renewable energy or other energy sources into electrical energy) has several issues. One of the issues during the connection of microgrids to the network is the presence of nonlinear loads, which are related to the structure of power electronics and other similar loads that are used in the network or the microgrid.

3. SIMULATION

3.1. Introduction

With the expansion of industries and population growth, the need for energy is increasing each day. Given the shortage of the energy generated from fossil fuels, the global community is paying more attention to renewable energy. Renewable energies are the energies that are obtained from sunlight and used in two fashions; the first is the use of solar thermal energy for domestic, industrial, and power plants, and the second is the direct conversion of light from the sun into electricity using PV solar cells. The main advantages of solar cells include free and pollution-free fuel, and the disadvantages are the high initial costs and low system efficiency. Each year, the cell production has higher yields and lower prices than the previous years, while low yields and relatively high prices per cell remain among the challenges of this technology. The main barriers to the use of this technology are the scientific and technical weakness in conversion due to the lack of knowledge and field experience, variable and alternating amounts of energy due to climatic and seasonal changes, and changes in the direction of radiation.

To exploit the available resources, mechanical systems are required to place solar panels in the direction of uninterrupted sunlight at any time; this method is known as a solar tracking system. Furthermore, an electronic system is essential to place the output of the solar panels at a suitable operating point with the maximum transmission power. However, the placement of solar panels at the point of maximum power may be problematic as in the non-linearity of the output characteristic of the solar cell and the variability of this characteristic in terms of light radiation and even cell temperature. Therefore, a system should be implemented for the control of solar cells along with the placement of solar cells at the optimal working point. In case of change in this point due to climatic conditions, the maximum transmission power of the system could be tracked continuously and rapidly, so that the solar cell would remain at the optimal point. This section simulates the proposed method for determining the MPPT of a solar array.

In the present study, we initially investigated the effects of temperature changes and radiation intensity on the MPPT value of solar arrays, followed by the effects of shadow on the performance of the solar arrays. In addition, the PSO, DE, and ICA random optimization algorithms were used to determine the MPPT of the solar at different temperatures, radiation intensities, and atmospheric conditions.

3.2. Climatic Conditions in Determining MPPT of Solar Arrays

In the current research, we evaluated the effects of climatic conditions on the MPPT of the solar arrays. As is shown in Figure 8, the solar cell was initially modeled in MATLAB Simulink environment. According to the findings, nonlinear, environmental solar cells (temperature and radiation) were dependent on the P-I and V-I characteristics. In addition, the working point of the solar cells depended on their charge attachment.

To recognize the behavior of a solar cell, a model with an electrical average should be developed based on separate electrical components with well-established behavior. An ideal solar cell is modeled with a current source parallel to a diode although no solar cell is practically ideal. In the present study, we added a sub-resistor and a series resistor to the model. Table 1 shows the basic characteristics of these cells at the temperature of 25°C.

Table 1 characteristics of silicon solar cells arrays in T=25 ℃

Current -Temperature Coefficient	$\alpha = 0.002086(\frac{A}{^{\circ}C})$
Voltage-Temperature Coefficient	$\beta = 0.0779(\frac{V}{^{\circ}C})$
Reverse Saturation Current	$I_o = 0.5 \times 10^{-4}\ (A)$
Short Circuit	$I_{SC} = 4.8\ (A)$
Solar resistor	$R_S = 0.0277(\Omega)$
Coefficient Solar	$\lambda = 20.41(V^{-1})$

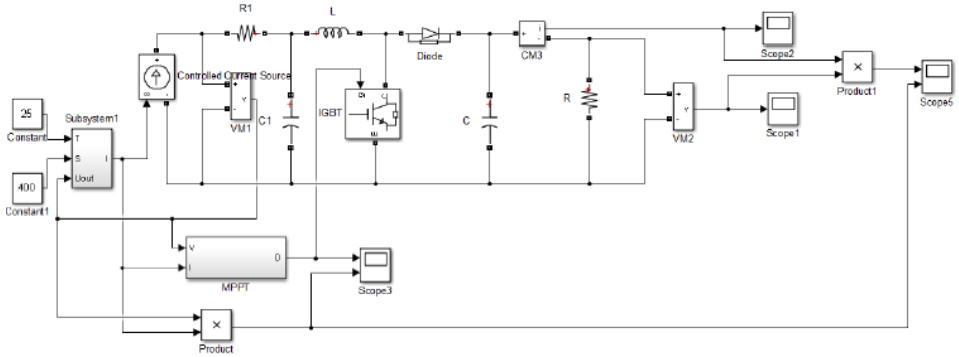

Fig. 8 Solar Photovoltaic Modeling

Figures 9 and 10 show that at the temperature of 25°C and radiation intensity of 1,000 W/m2, the solar array had 4.55 A, voltage of 7.59 V, and power of 34.54 MPPT watts. Notably, only one MPP point was observed since there was no shadow conditions in the solar array.

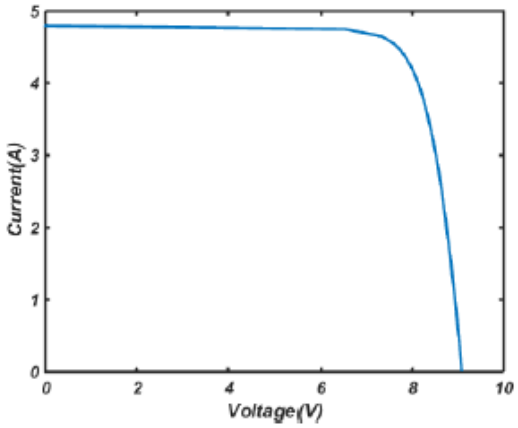

Fig. 9 Curve I-V (T=25℃, Radiant intensity $S = 1000\frac{W}{m^2}$)

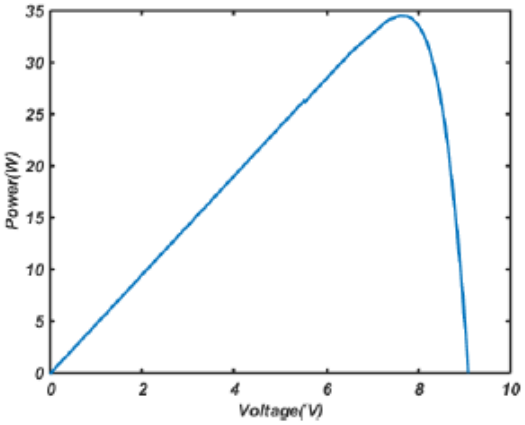

Fig. 10 Curve P-V (T=25℃, $S = 1000 \frac{W}{m^2}$)

Figure 11 shows the effects of the changes in radiation intensity on the MPP of the solar arrays at the temperature of 25°C. As can be seen, the decreased intensity of radiation in the solar arrays led to the reduction of the maximum power of the solar arrays. Figure 12 depicts the effects of changes in the MPP of the solar arrays at the radiation intensity of 1,000 W/m2. As is observed, the increased temperature of the solar arrays led to the reduction of the maximum power of the solar arrays.

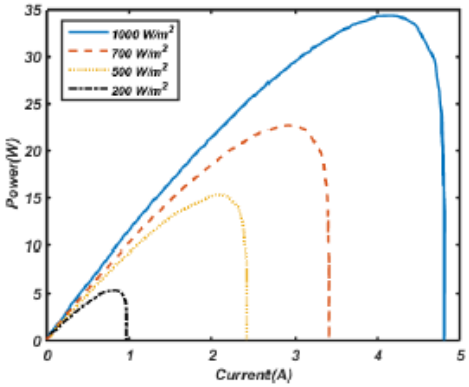

Fig. 11 Curve P-I
(T = 25℃, varied radiant intensity)

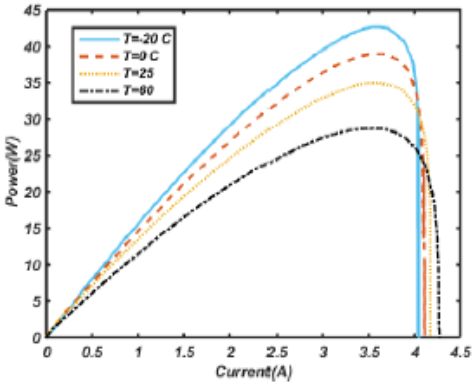

Fig. 12 Curve P-I
($S = 1000 \frac{W}{m^2}$, varied temperature)

3.3. Determining MPPT of Solar Arrays with Partial Shading

Partial shadowing is performed by the shadows created by buildings, trees, and clouds (moving shadows). As a result of creating a shadow instead of the maximum power point, several peaks were observed in the voltage-current characteristic of the module in the

present study. With regard to the moving shadow conditions, the photovoltaic system module is typically divided into three sections (Figure 13).

In the current research, radiation and facade data were collected in each section and used with a sample photovoltaic system in MATLAB software to calculate the short-circuit current and open-circuit voltage in the module section. The data were fed to random algorithms to calculate the maximum power point section voltage and the maximum power point current. With the changes in the radiation and temperature in section i, the values of Isc and Voc also changed. Therefore, the appropriate function was automatically adjusted, acting to find the new value of the maximum power point of this section. It was assumed that the S radiation and temperature conditions of the section remained unchanged, and the maximum power point of the same section was searched by a random algorithm.

After obtaining the maximum power point values of each independent section, the maximum power point of the entire module of the photovoltaic system was measured by the instantaneous possible mean of the maximum power point obtained from each module section of the photovoltaic system. The process was repeated in case of any changes in the radiation of each section of the module.

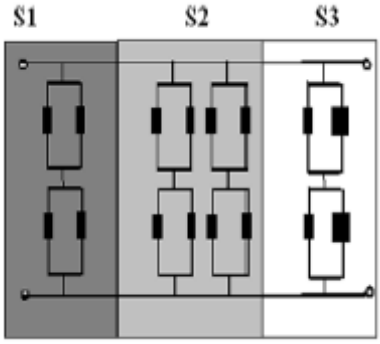

Fig. 13 Solar Array Module with Different Radiation Intensities

In this section, the MPP of the solar arrays was initially determined under shadow conditions. For this purpose, two scenarios were also tested, the details of which are presented in Table 2. As is depicted in Figures 14-17, a local number was created in the solar array under optimal shadow conditions, making it impossible to search for MPP in the solar array using conventional methods.

Table 2 Two Scenarios under Shadow Conditions

Radiant intensity	W/m^2	W/m^2
Cell1	1000	1000
Cell2	300	600
Cell3	200	260

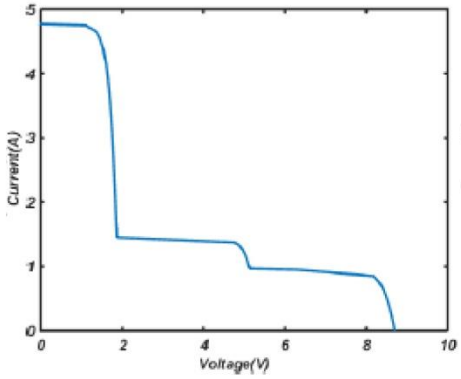

Fig. 14 Curve I-V (T=25℃; first case)

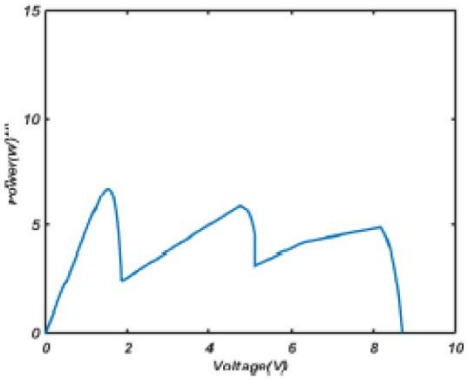

Fig. 15 Curve P-V (T=25℃; first case)

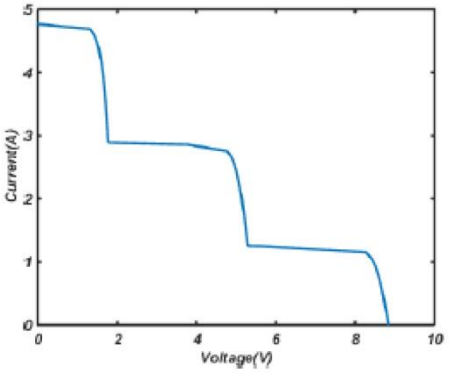

Fig. 16 Curve I-V (T=25℃; second case)

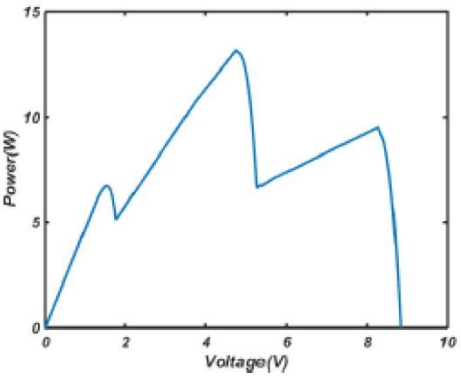

Fig. 17 Curve P-V (T=25℃; second case)

3.4. Determining MPPT Using Random Algorithms

In the studied system, the maximum power point detector connected the module of the photovoltaic system to the battery. The maximum power point tracker consisted of a DC-DC boost converter and a control system (maximum power point tracking by random algorithms). In general, the maximum power point tracking unit of random algorithms uses random parameters in the inputs to determine the current and voltage based on the maximum power through equations.

In the present study, the inputs of the maximum power point tracking unit were random algorithms for cell temperature, solar radiation, and the number, temperature, and radiation of the cells in the shade. The maximum power point detector adjusted the operating point of the solar array for the maximum power by adjusting the boost converter life cycle. The optimization algorithms had two modes with three scenarios in each case, which were defined to determine the maximum power point of the solar arrays. The defined modes are shown in Tables 3 and 4. In these cases, the number of the cells in the shade, their temperature, and radiation intensity differed in each scenario.

Table 3 Basic Conditions of Solar Arrays in Assessment of Random Algorithms in First Case

	Scenario 1	Scenario 2	Scenario 3
Number of cells in non-shady conditions	40	30	20
Cell temperature in non-shady conditions	25	25	25
Intensity of cell radiation in non-shady conditions	900	900	900
Number of cells in shade	0	10	20
Cell temperature in shade	0	20	20
Intensity of cell radiation in shade	0	500	500

Table 4 Basic Conditions of Solar Arrays in Assessment of Random Algorithms in Second Case

	Scenario 1	Scenario 2	Scenario 3
Number of cells in non-shady conditions	50	40	35
Cell temperature in non-shady conditions	30	30	30
Intensity of cell radiation in non-shady conditions	750	750	750
Number of cells in shade	0	10	15
Cell temperature in shade	0	25	25
Intensity of cell radiation in shade	0	600	600

Tables 5-7 show the basic parameters of the PSO, DE, ICA algorithms. In all these algorithms, the number of the iterations, number of the control parameters (population dimension), and initial population were equal.

Table 5 Parameters of DE Algorithm

Parameter	Value
Population Size	10
Number of Dimensions of Each Population	1
Number of Repetitions	50

Table 6 Parameters of PSO Algorithm

Parameter	Value
Population Size	10
Number of Dimensions of Each Population	1
Number of Repetitions	50
W Max.	0 and 9
W Min.	0 and 3
C1	2 and 05
C2	2 and 05

Table 7 Parameters of ICA Algorithm

Parameter	Value
Population Size	10
Number of Dimensions of Each Population	1
Number of Repetitions	50
Number of Empires	2

Figures 18-20 depict the speed and convergence of the PSO, DE, and ICA algorithms in the first case, and the second case is shown in Figures 21-23. As can be seen, the convergence speed of the ICA algorithm was moderately higher compared to the other algorithms. Notably, these algorithms are based on random numbers, and their convergence rate may change each time the program is run. According to our findings, the speed of the training-based algorithm was higher than the other algorithms. In addition, the optimal point was obtained accurately in all the repetitions.

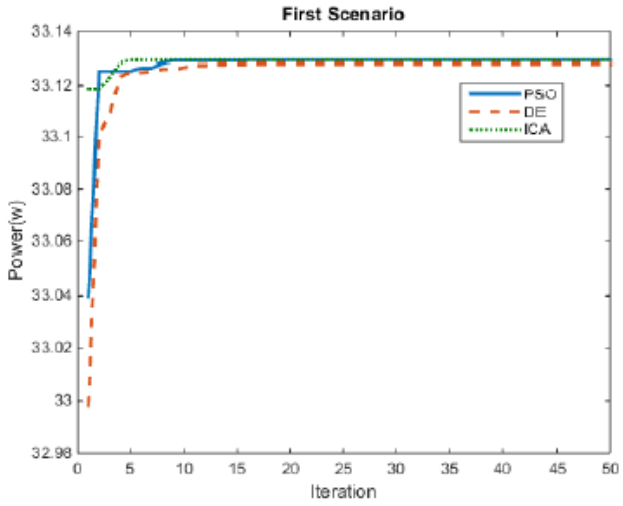

Fig. 18 Function of Random Algorithm in Determining MPPT (mode 1, scenario 1)

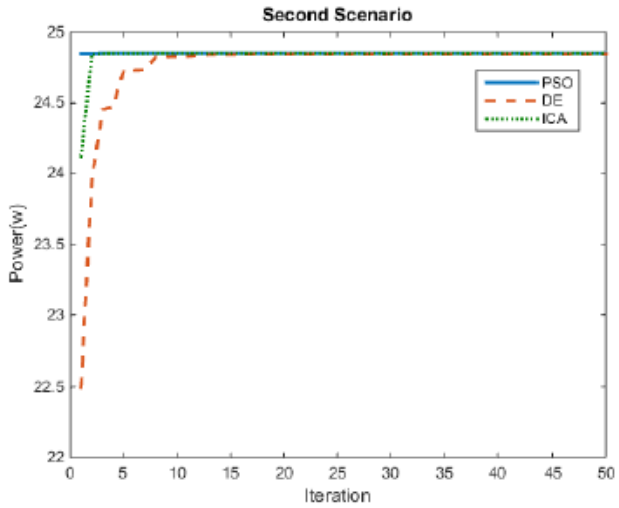

Fig. 19 Random Algorithm Performance in Determining MPPT (mode 1, scenario 2)

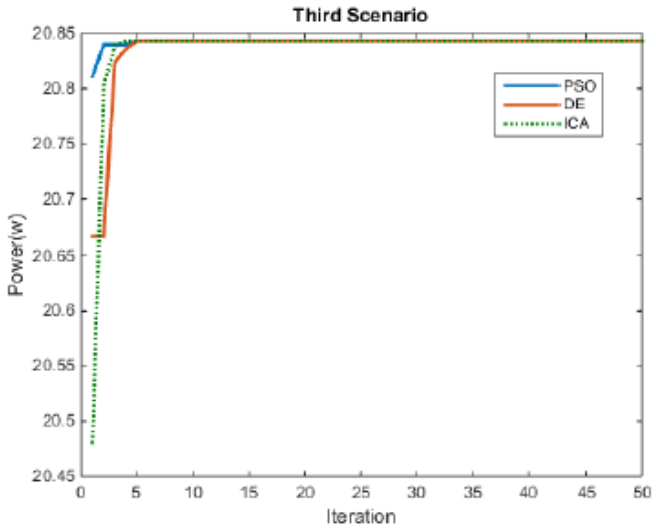

Fig. 20 Performance of Random Algorithm in Determining MPPT (mode 1, scenario 3)

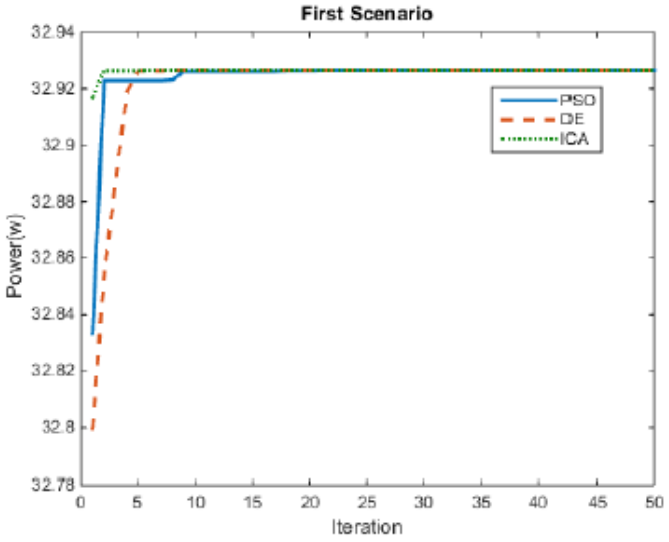

Fig. 21 Performance of Random Algorithm in Determining MPPT (mode 2, scenario 1)

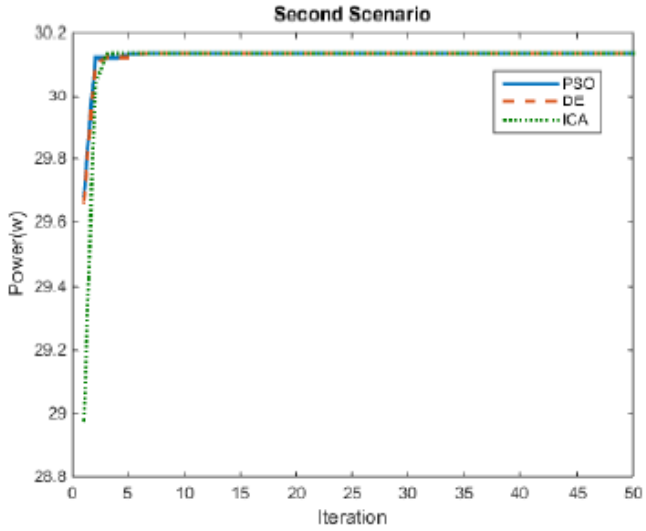

Fig. 22 Performance of Random Algorithm in Determining MPPT (mode 2, scenario 2)

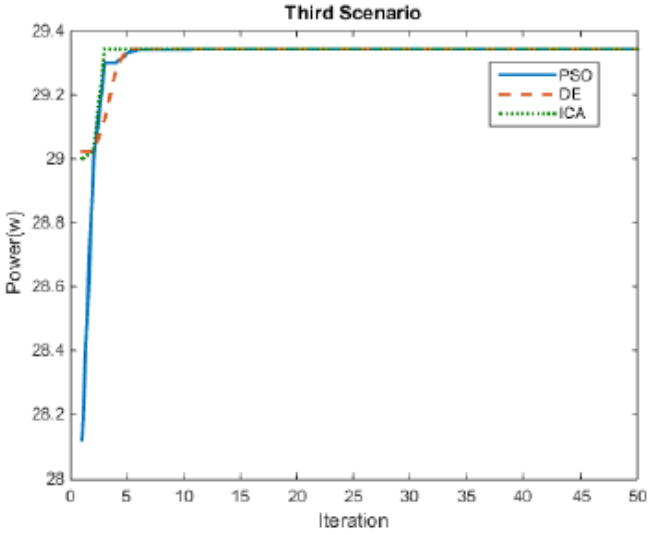

Fig. 23 Performance of Random Algorithm in Determining MPPT (mode 2, scenario 3)

As can be seen, the accuracy and performance of the proposed method were evaluated using a photovoltaic system consisting of a solar panel, DC/DC converter, battery, and control system (MPPT), which was simulated using MATLAB Simulink software. Furthermore, three stochastic optimization algorithms (PSO, DE, and ICA) were utilized to compare the performance of the MPPT. To evaluate the performance, efficiency, and accuracy, the method was compared with the VMPPT, P&O, and CMPPT methods similar to the previous paper in this regard.

3.5. MPPT based on Perturb and Observe (P&O) Algorithm [32-33]

The P&O method has been widely used for MPPT given its convenience. In a typical P&O algorithm, the operating point voltage of the solar array is disturbed in one direction to observe the resulting output power. If the power change is positive, the operating point of the system has moves to the MPP point, and the voltage must be disturbed again in the same direction. If the power changes are negative, the operating point must be moved away from this point, and the voltage will change in the opposite direction of the first disturbance (Figure 24).

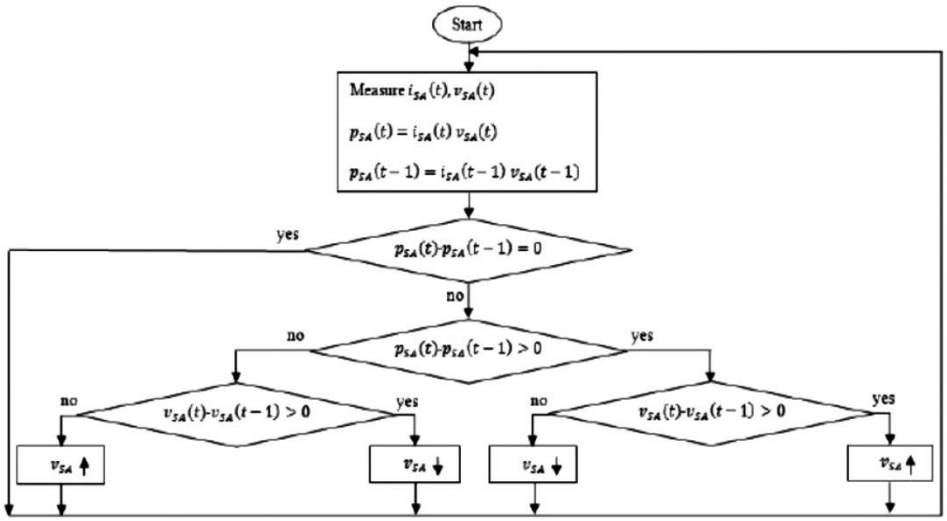

Fig. 24 P&O method

3.6. MPPT Based on Voltage (VMPPT) [34-36]

In VMPPT, the correlation between the output voltage of the cellular array (V_{SA}) is the same as V_{mp}, and the open-circuit voltage (V_{OC}) is considered linear.

$$V_{mp} = K_v V_{OC} \tag{15}$$

In the equation, *Kv* is a constant known as the voltage coefficient. Figure 25 shows the value of $Kv=V_{mp}/V_{OC}$ based on different temperatures and radiation conditions where Nshade is equal to 10, 15, 20, and 25, respectively. Based on these results, it is clear that the *Kv* value is not fixed, and the VMPPT method is erroneous in shady conditions. The algorithm of this method is depicted in Figure 26.

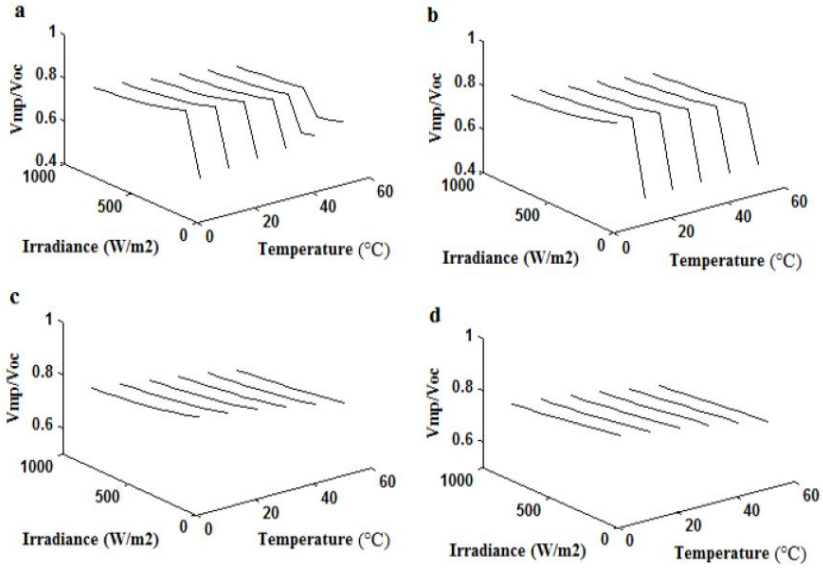

Fig. 25 Voltage Coefficient Calculated in Different Temperature and Radiation Intensity Conditions; a) 10 Shaded Cells, b) 15 Shaded Cells, c) 20 Shaded Cells, d) 25 Shaded Cells [34-36]

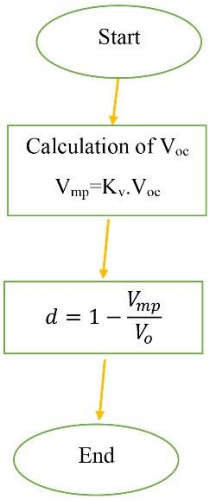

Fig. 26 VMPPT Method Algorithm [34-36]

3.7. MPPT Based on Current (CMPPT) [34-36]

In CMPPT, the correlation between the output current of a cellular array (I_{SA}, which is *Imp*), and its short circuit current (I_{sc}) is considered linear.

$$i_{mp} = K_i i_{sc} \tag{16}$$

In the equation, K_i shows known as the current coefficient. Figure 26 shows the value of $K_i = i_{mp} / i_{sc}$ based on different temperature and radiation conditions where Nshade is equal to 10, 15, 20, and 25, respectively. Based on these results, it is clear that the K_i value is not fixed, and the CMPPT method is erroneous in shady conditions. The algorithm of this method is shown in Figure 27.

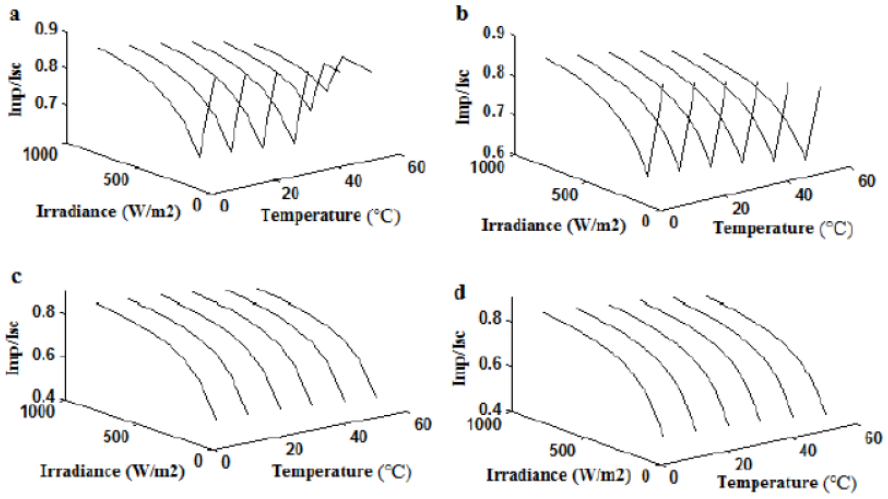

Fig. 26 Coefficient Calculated in Different Temperature and Radiation Intensity Conditions; a) 10 Shaded Cells, b) 15 Shaded Cells, c) 20 Shaded Cells, d) 25 Shaded Cells [34-36]

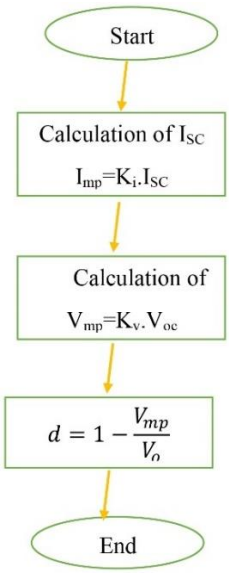

Fig. 27. CMPPT Method Algorithm [34-36]

3.8. MPPT Based on artificial neural network [37-38]

The method presented in this study provides a two-stage maximum power tracking method that determines the maximum point for two modules having serial connection. In the first step, the radiation and the temperature of the array is measured and the final P–I curve is found. Then, a search algorithm is implemented to approximate the MPP location with two current and power parameters at the MPP point [37-38]. When the weather conditions exceed beyond a certain level, the search is repeated. In the second step, the actual characteristic curve starts the search for MPP from the estimated point in the first stage or from its previous performance point, which depends on changes in the performance conditions. In one such case, P and O and RCC methods are used to perform the second phase of this algorithm, and the neural network is realized, correspondingly [37-38].

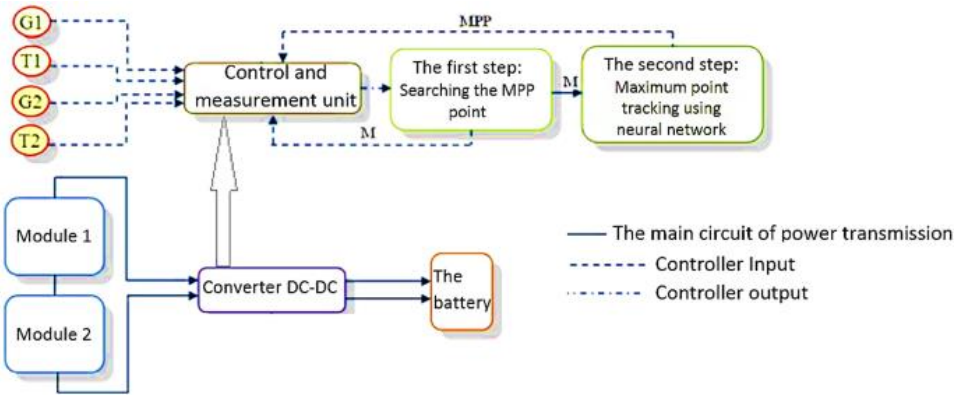

Fig. 28 The schematic diagram of the proposed approach [37]

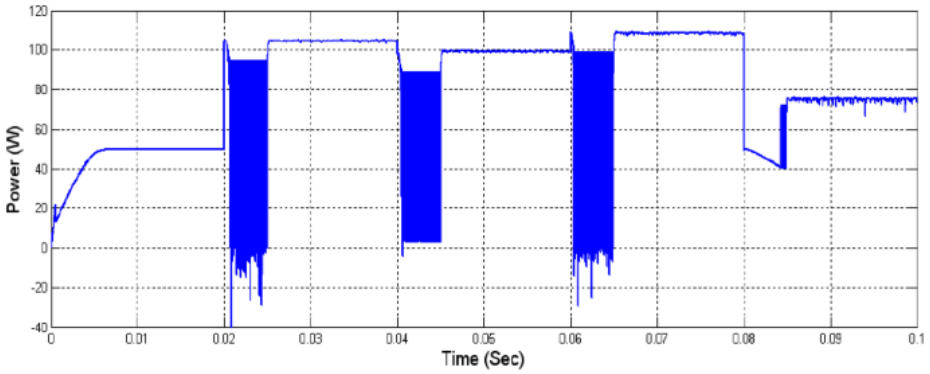

Fig. 29 The power of the PV array in the first simulation [37]

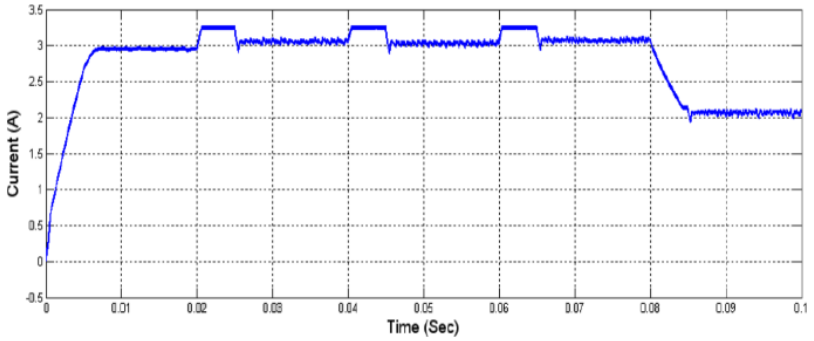

Fig. 30 The current of the PV array in the first simulation [37]

The comparison of the obtained results showed that this method has two steps and therefore is not faster than our methods, and also does not guarantee system stability.

3.7. MPPT Based on Fuzzy Logic [39-40]

The change in the duty cycle is done by Fuzzy logic controller by sensing the power output of the solar panel. The proposed controller is aimed at adjusting the duty cycle of the DC-DC converter switch to track the maximum power of a solar cell array. The inputs to the fuzzy logic system will be error (E) and Change in Error (C). The output will be the Change in Duty Cycle (dD) at sampling instant k [40]. The fuzzy logic consists of the following stages: fuzzification, rule base, inference system and defuzzification. The Fuzzy variables are divided into 5 linguistic hedges: Negative Big (NB), Negative Small (NS), Zero (ZE), Positive Small (PS) and Positive Big (PB).The membership functions are chosen as shown in Fig 31. Fig. 32 & Fig. 33 show that the linguistic hedges of change in error and change in duty cycle respectively. The result is shown in Fig.34.

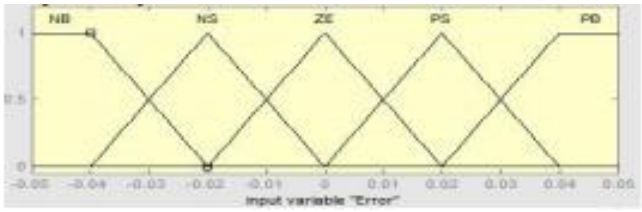

Fig. 31 Linguistic hedges of change in error [39]

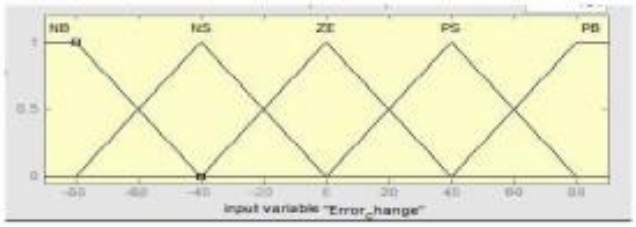

Fig. 32 Linguistic hedges of change in error [39]

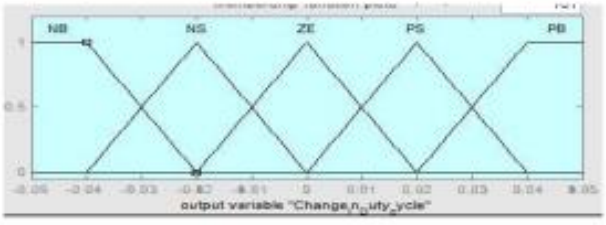

Fig. 33 Linguistic hedges of change in duty cycle [39]

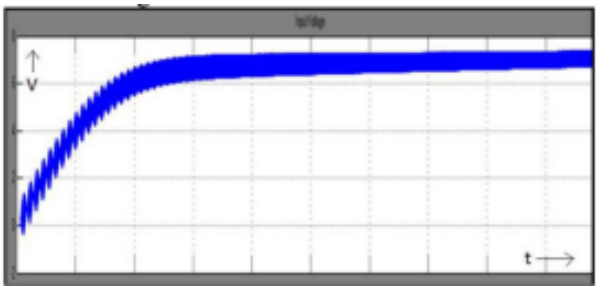

Fig. 34 Output voltage of the solar panel without MPPT

As you can see, shadow conditions are not considered in this method.

The comparison of the obtained results (Section 3-4) with the findings of other studies (Sections 3-5 to 3-9) indicated that the use of stochastic optimization algorithms is superior to other methods as they are not erroneous in shady conditions.

4. CONCLUSION

In the implementation of the network in this study, the load was considered a point load, and all the solar panels were centrally simulated. In other words, the cloud passage affected all the solar panels similarly, and the implemented network became centralized. This approach is common in industrial and power plants and for domestic use, while the industrial use is more frequent compared to the domestic use since residential areas often lack the necessary space to build a centralized solar power plant.

In industrial areas, energy storage devices (e.g., batteries) must be used to compensate for the voltage drop applied to the system, which may in turn cause islanding and load interruption. These batteries, albeit temporarily, allow the photovoltaic system to compensate for the microgrid power shortage locally, thereby eliminating the need for the network to compensate for the power shortage. As a result, the voltage drop does not occur due to the current influx in the network.

In this study, a control system was designed to control the high-penetration solar power plants in the network. Furthermore, infiltration was obtained at different loads, and the effects of cloud transit on the system were also simulated and obtained. The results of these simulations are as follows:

1. The characteristics of a solar array depend on atmospheric conditions (e.g., temperature and radiation intensity).

2. In non-shady conditions, solar arrays have only one maximum power point, while some local optimal points could be observed in shady conditions. Consequently, it would be difficult to use conventional methods to determine the MPPT of solar arrays.

3. Stochastic optimization algorithms could be used to determine the MPP point of solar arrays in proper shadow conditions. In this study, three algorithms (DE, PSO, and ICA) were employed to determine the MPPT of the solar arrays in shady conditions, and the speed of the colonial competition algorithm was observed to be higher compared to the other algorithms.

REFERENCES

[1] S. Chalmers, M. Hitt, J. Underhill, P. Anderson, P. Vogt and R. Ingersoll, "The effect of photovoltaic power generation on utility operation", *IEEE Trans. Power Appar. Syst.*, vol. PAS-104, no. 3, pp. 524–530, March 2015.

[2] Y. Zhou, H. Li and L. Liu, "Integrated Autonomous Voltage Regulation and Islanding Detection for High Penetration PV Applications", IEEE Trans. Power Electron., vol. 28, no. 6, pp. 2826–2841, 2012.

[3] M. J. E. Alam, K. M. Muttaqi and D. Sutanto, "A Novel Approach for Ramp-Rate Control of Solar PV Using Energy Storage to Mitigate Output Fluctuations Caused by Cloud Passing", *IEEE Trans. Energy Convers.*, vol. 29, no. 2, pp. 507–518, March 2014.

[4] W. T. Jewell, R. Ramakumar and S. R. Hill, "A study of dispersed photovoltaic generation on the PSO system", *IEEE Trans. Energy Convers.*, vol. 3, no. 3, pp. 473–478, Sept. 1988.

[5] H. Asano, K. Yajima, Y. Kaya, "Influence of photovoltaic power generation on required capacity for load frequency control". *IEEE Trans. Energy Convers.*. vol. 11, no. 1, pp. 188–193, March 1996.

[6] S. A. Pourmousavi, A. S. Cifala and M. H. Nehrir. "Impact of high penetration of PV generation on frequency and voltage in a distribution feeder" In Proceedings of the North American Power Symposium (NAPS), IEEE, 2017, pp. 1–8.

[7] M. E. Baran, H. Hooshyar, Z. Shen and A. Huang, "Accommodating High PV Penetration on Distribution Feeders", *IEEE Trans. Smart Grid*, vol. 3, no. 2, pp. 1039–1046, June 2012.

[8] Guest Editorial, "Progress in ElectricMachines, Power Converters and their Control for Wave Energy Generation", *IET Electr. Power Appl.*, vol. 14, no. 5, April 2020.

[9] N. Patapoff and D. Mattijetz, "Utility interconnection experience with an operating central station MW-Sized photovoltaic plant", *IEEE Trans. Power Appar. Syst.*, vol. PAS-104, no. 8, pp. 2020–2024, Aug. 1985.

[10] D. Cyganski, J. Orr, A. Chakravorti, A. Emanuel, E. Gulachenski, C. Root and R. C. Bellemare, "Current and voltage harmonic measurements at the Gardner photovoltaic project", *IEEE Trans. Power Deliv.*, vol. 4, no. 1, pp. 800–809, Jan. 1989.

[11] M. H. Moradi and A. R. Reisi, "A hybrid maximum power point tracking method for photovoltaic systems". *Sol. Energy*, vol. 85, no. 11, pp. 2965–2976, Nov. 2011.

[12] Z.-D. Zhong, H.-B. Huo, X.-J. Zhu, G.-Y. Cao, Y. Ren, "Adaptive maximum power point tracking control of fuel cell power plants", *J. Power Sources*, vol. 176, no. 1, pp. 259–269, Jan. 2008.

[13] Photovoltaics and Distributed Generation, www.fsec.ucf.edu

[14] F. Antony, C. Durschner, K. H. Remmers, *Photovoltaic For Professionals: Solar Electric Systems Marking, Design And Installation*. Routledge, 2007.

[15] European Photovoltaic Industry Association, *Market Report 2011*. 2012.

[16] P. Pereira da Silva, G. Dantas, G. Ivan Pereira, L. Câmara, N. J. De Castro, "Photovoltaic distributed generation – An international review on diffusion, support policies, and electricity sector regulatory adaptation", Renew. Sust. Energy Rev., vol. 103, pp. 30–39, April 2019.

[17] P. Chaudhary and M. Rizwan "Energy management supporting high penetration of solar photovoltaic generation for the smart grid using solar forecasts and pumped hydro storage system", *Renew. Energy*, vol. 118, pp. 928–946, April 2018.

[18] A. Mohapatra, B. Nayak, P. Das and K. Barada-Mohanty, "A review on MPPT techniques of PV system under partial shading condition", *Renew. Sust. Energy Rev.*, vol. 80, pp. 854–867, Dec. 2017.

[19] J. Gosumbonggot and G. Fujita, "Partial Shading Detection and Global Maximum Power Point Tracking Algorithm for Photovoltaic with the Variation of Irradiation and Temperature", *Energies*, vol. 12, no. 2, pp. 1–22. Jan. 2019.
[20] M. Premkumar and R. Sowmya, "An effective maximum power point tracker for partially shaded solar photovoltaic systems", *Energy Rep.*, vol. 5, pp. 1445–1462, Nov. 2019.
[21] J. Qi, Y. Zhang and Y. Chen," Modeling and maximum power point tracking (MPPT) method for PV array under partial shade conditions", *Renew. Energy*, vol. 66, pp. 337–345, June 2014.
[22] B. Liu, K. Li, D. D. Niu, Y. A. Jin and Y. Liu, "The characteristic analysis of the solar energy photovoltaic power generation system", In Proceedings of the 5th Global Conference on Materials Science and Engineering, IOP Conf. Series: Materials Science and Engineering, 2017, vol. 164, p. 012018.
[23] S. Dubey, J. Narotam-Sarvaiya and B. Seshadri, "Temperature Dependent Photovoltaic (PV) Efficiency and Its Effect on PV Production in the World – A Review", *Energy Procedia*, vol. 33, pp. 311–321, 2013.
[24] X.-S. Yang, *Nature-Inspired Optimization Algorithms.* Science Direct, 2014.
[25] B. Seixas Gomes de Almeida and V. C. Leite. "Particle Swarm Optimization: A Powerful Technique for Solving Engineering Problems" in *Swarm Intelligence - Recent Advances, New Perspectives and Applications*. IntechOpen, 2019.
[26] P. Rocca, G. Oliveri and A. Massa, "Differential Evolution as Applied to Electromagnetics", *IEEE Antennas Propag. Mag.*, vol. 53, no. 1, pp. 38–49, Feb. 2011.
[27] R. Storn and K. Price, "Differential evolution - a simple and efficient heuristic for global optimization over continuous spaces". *J. Glob. Optim.*, vol. 11, no. 4, pp. 341–359, Dec. 1997.
[28] R. Storn, "On the usage of differential evolution for function optimization", In Proceedings of the Biennial Conference of the North American Fuzzy Information Processing Society (NAFIPS), 1996, pp. 519–523.
[29] E. Atashpaz-Gargari and C. Lucas, "Imperialist Competitive Algorithm: An algorithm for optimization inspired by imperialistic competition" In Proceedings of the IEEE Congress on Evolutionary Computation, 2007, pp. 4661–4666.
[30] S. Hosseini and A. Al Khaled, "A survey on the Imperialist Competitive Algorithm metaheuristic: Implementation in engineering domain and directions for future research", *Appl. Soft Comput.*, vol. 24, pp. 1078–1094, Nov. 2014.
[31] A. Majzoobi and A. Khodaei, "Application of Microgrids in Supporting Distribution Grid Flexibility", *IEEE Trans. Power Syst.*, vol. 32, no. 5, pp. 3660–3669, Sept. 2017.
[32] J. Ahmed and Z. Salam, "An improved perturb and observe (P&O) maximum power point tracking (MPPT) algorithm for higher efficiency", *Appl. Energy*, vol. 150, pp. 97–108, July 2015.
[33] M. A. Elgendy, B. Zahawi and D. J. Atkinson, "Evaluation of perturb and observe MPPT algorithm implementation techniques", In Proceedings of the 6th IET International Conference on Power Electronics, Machines and Drives, 2012, pp. 1–6.
[34] M. A. S. Masoum and M. Sarvi, "Voltage and current based MPPT of solar arrays under variable insolation and temperature conditions" In Proceedings of the 43rd International Universities Power Engineering Conference, 2008, pp. 1–5.
[35] M. A. S. Masoum, H. Dehbonei and E. F. Fuchs, "Theoretical and experimental analyses of photovoltaic systems with voltageand current-based maximum power-point tracking", *IEEE Trans. Energy Convers.*, vol. 17, no. 4, pp. 514–522, Dec. 2002.
[36] M. Veerachary, T. Senjyu and K. Uezato, "Voltage-Based Maximum Power Point Tracking Control of PV System", *IEEE Trans. Aerosp. Electron. Syst.*, vol. 38, no. 1, pp. 262–270, Jan. 2002.
[37] Z. Zandi and A. H. Mazinan, "Maximum power point tracking of the solar power plants in shadow mode through artificial neural network", *Complex Intell. Syst.*, vol. 5, pp. 315–330, Oct. 2019.
[38] Syafaruddin, E. Karatepe and T. Hiyama, "Artificial neural network-polar coordinated fuzzy controller based maximum power point tracking control under partially shaded conditions", *IET Renew. Power Gener.*, vol. 3, no. 2, pp. 239–253, May 2009.
[39] R. Mahalakshmi, A. Aswin Kumar and A. Kumar," Design of Fuzzy Logic Based Maximum Power Point Tracking Controller for Solar Array for Cloudy Weather Conditions", In Proceedings of the Power and Energy Systems: Towards Sustainable Energy (PESTSE), 2014, pp. 1–4.
[40] M. S. Cheik, C. Larbes, G. F. Kebir and A. Zerguerras, "Maximum power point tracking using a fuzzy logic control scheme", *Revue des Energies Renouvelables*, vol. 10, no. 32, pp 387–395, Sept. 2007.